

A New Data Transformation Method for Cbers-02b Multi-spectral Images

Chengwen Zhang^{a,b}, Jiakui Tang^{a*}, Sujuan Mi^{a,b}, Lijun Zhao^{a,b},
Yongzhi Li^{a,b}, Xinju Yu^{a,b}

^aKey Laboratory of Coastal Zone Environmental Processes, CAS; Shandong Provincial Key Laboratory of Coastal Zone Environmental Processes, Yantai Institute of Coastal Zone Research, Chinese Academy of Sciences, Yantai, 264003, P. R. China

^bGraduate University of Chinese Academy of Sciences, Beijing, 100049, P. R. China

* Corresponding author. Lab of Information Integrations and Applications, Yantai Institute of Coastal Zone Research, Chinese Academy of Sciences, China, Tel.: +86 0535 2109194; fax: +86 0535 2109194.

E-mail addresses: jktang@yic.ac.cn; cwzhang123@163.com

Keywords: Remote sensing; LBV transformation ;multi-spectral images;classification; CBERS-02B

Abstract. According to the detailed studies on the data of China-Brazil earth resources satellite-02B (CBERS-02B) and the LBV data transform method proposed by the previous researcher, a new LBV data transformation equations for CBERS-02B data was specially proposed. A transformation experiment on CBERS-02B data showed that the LBV transformed result images were more vivid, and the features of result images were more easily to be classified than the fault color composite images of original bands. In order to evaluate the performance of this proposed method, the maximum likelihood supervised classification method was used. The final classification results showed that the accuracy of the LBV transformed image is obviously better than that of the fault color composite images of original bands, which demonstrated that the proposed LBV transformation method for CBERS-02B has good potential for CBERS-02B data in the future applications.

1. Introduction

The China-Brazil earth resources satellite-02B (CBERS-02B) was launched successfully on September 19, 2007, which is developed by the collaboration between China and Brazil on the project of an earth resources satellite. This satellite payloads three sensors: the CCD cameras, including five channels of wave-length from 0.42~0.89 μm , and spatial resolution 19.5 meters; the high resolution cameras (HR), 0.5~0.8 μm , 2.36 meters, and the wide field imager (WFI), two channels, 0.63~0.89 μm , 258 meters. The multi-spectral images of CBERS-02B are good data sources for remote sensing applications.

In order to effectively extract useful information from CBERS-02B images, many traditional methods can be used, such as PCA (principal components analysis) [1], HIS (intensity, hue, saturation) [2-7], filtering processes including high-pass filtering and low-pass filtering. However, most of these methods only process three original bands to get new integrated images; which result into that the spectral information of the entire four multi-spectral bands can not be fully used.

The LBV data transformation method proposed by Zeng in 2007 [8] is a new method of data transformation. The method can be used to extract the general radiance level L , the visible-infrared radiation balance B and the band radiance variation vector (direction and speed) V from Four multi-spectral bands of original satellite images to generate high quality LBV color composite images. The result LBV image can be well used for classification and digital analysis of ground features [8].

Although the LBV data transformation method has been proved to be of high performance for 3 or 4 bands of SPOT, IKONOS and Quick Bird images and also can be extended to 5 bands of NOAA and 7 bands of TM images, it is can not be directly used for the new CBERS-02B data because the transformation is relied on the specified sensor data. Therefore, the special LBV **transformation** equations for CBERS-02B multi-spectral images were studied and proposed in this paper.

2. Transformation method

According to the LBV **transformation** procedure proposed by Zeng [8], regression method was used to extract information from satellite images. The main detailed procedures for CBERS-02B are described as follows.

2.1 Linear and Quadratic Regression Equations

For CBERS-02B images, the quadratic and linear regression equations as follows:

$$\hat{D} = a + b\lambda + c\lambda^2 \quad (1)$$

$$\hat{D} = a + b\lambda \quad (2)$$

In equations (1) and (2), \hat{D} is the regressive estimation of D and D is the original grey-level value of the ground feature in a CBERS-02B band; λ is the selected wavelength value for the band; a, b and c are the regression equation coefficients to be evaluated. V_i is defined as the regressive residual:

$$V_i = \hat{D}_i - D_i \quad (3)$$

The independent variable values have been selected as $\lambda_1=0.48\mu\text{m}$, $\lambda_2=0.56\mu\text{m}$, $\lambda_3=0.66\mu\text{m}$, $\lambda_4=0.83\mu\text{m}$, respectively. The coefficients a, b and c of the quadratic regression equations can be calculated by the method proposed by Zeng (2007) [8]:

$$a = 10.253117D_1 - 3.635050D_2 - 10.453690D_3 + 4.835624D_4 \quad (4)$$

$$b = -29.363121D_1 + 13.328764D_2 + 33.401918D_3 - 17.367561D_4 \quad (5)$$

$$c = 20.543140D_1 - 10.896957D_2 - 24.987769D_3 + 15.341586D_4 \quad (6)$$

For the linear regression equation, the coefficients a, b can be obtained by the same method:

$$a = 1.662761D_1 + 0.921640D_2 - 0.004760D_3 - 1.579641D_4 \quad (7)$$

$$b = -2.233614D_1 - 1.061882D_2 + 0.402783D_3 + 2.892713D_4 \quad (8)$$

2.2 Definiton Expression of V and the Calculation Equation for CBERS-02B Images

In order to analyze the data of CBERS-02B, several images were chosen to be classified into nine typical ground cover features. The respective grey value of each ground feature was obtained by averaging the grey values of ground cover pixel samples. The grey level values of each typical ground feature were described in Table 1. Fig.1 (a) is the curves of the grey level values of ground features in table1.

All quadratic and linear regression equations can be calculated according to the above a, b and c expressions, and the regression curves and lines for ground features were shown in Fig.1 (b) and (c). Simultaneously, the regression residual values are then fixed. Fig.2 (a) shows the broken line, quadratic regression curves and regression residuals v_1, v_2, v_3 and v_4 of a vegetation and a bare land i.e. the vegetation III: sparse (7) and the bare land II : quarry (9) in Fig.1.

It can be seen that the variation directions of the bared land (broken line 9) and the vegetation (broken line 7) are obviously opposite. Furthermore, the magnitude of the absolute value of residuals indicates the radiance variation's speed.

Meaningfully, the regression residuals can be a measure of the land radiance variation direction and speed (vector) V. Considering that only one variable can be used; the sum of these four variables v is the best choice. The variable V can be defined as follows:

$$\begin{aligned} V &= v_1 - v_2 + v_3 - v_4 \\ &= -0.571986D_1 + 1.334635D_2 - 0.942095D_3 + 0.179447D_4 \end{aligned} \quad (9)$$

2.3 Quadratic Regression Evaluated D value at $\lambda=0.62 \mu\text{m}$ as the General Radiance Level L

According to lots of experiments it was found that the quadratic regression-evaluated D value at $\lambda=0.62\mu\text{m}$ is the best variable to represent the general radiance level L when the 4th band CBERS-2B multiply by factor value 4. Therefore, the following equations were obtained to calculate the general radiance level L:

$$\begin{aligned} \hat{L} = D_{0.62} &= a + 0.62b + 0.62^2c \\ &= -0.055235D_1 + 0.439993D_2 + 0.650201D_3 - 0.139835D_4 \end{aligned} \quad (10)$$

2.4 The Slope Value of the Linear Regression Line as the Visible-infrared Radiation Balance B

The linear regression curves of the nine represent ground features are showed in Fig.2 (b). It can be found that the slopes of regression lines of the water with the abscissa axis are negative and greater, while the slopes of regression lines of the vegetation with the abscissa axis are positive and greater. Moreover, the slopes of the bare lands and towns are smaller than that of vegetation and larger than that of water. Therefore, it is highly recommended to define the minus slope value of the regression line as the visible-infrared radiation balance B. In this case, the water body has the greatest B value and hence has the bluest color on color composites if B image is assigned with blue in composition.

The following formula has been obtained to calculate the visible-infrared radiation balance B:

$$\begin{aligned} B &= -b \\ &= 2.233614D_1 + 1.061882D_2 - 0.402783D_3 - 2.892713D_4 \end{aligned} \quad (11)$$

2.5 Collection of the Information Extraction Equations of the L, B and V for CBERS-02B Images

It is convenient to collect the above mentioned three most important equations altogether as follows:

$$L_0 = -0.055235D_1 + 0.439993D_2 + 0.650201D_3 - 0.139835D_4 \quad (12)$$

$$B_0 = 2.233614D_1 + 1.061882D_2 - 0.402783D_3 - 2.892713D_4 \quad (13)$$

$$V_0 = -0.571986D_1 + 1.334635D_2 - 0.942095D_3 + 0.179447D_4 \quad (14)$$

The L, B and V are subscripted with 0 to emphasize that the L, B and V here are the initial values. The other forms of L, B and V will be introduced in the next section.

3. Transformation experiments

Four bands of CBERS-2B images, B01 (0.45-0.52 μ m), B02 (0.52-0.59 μ m), B03 (0.63-0.69 μ m) and B04 (0.77-0.89 μ m) bands, were used in **transformation** experiment, which were acquired on November 2, 2007, and the latitude and longitude of the subset images are 37°6'53"N, 121°49'E for upper left; 37°5'21"N, 121°7'50"E for lower right, respectively.

First of all, the initial equations (12)-(14) were used to transform the B01, B02, B03 and B04 bands. Then the result images V_0 , B_0 and L_0 can be obtained. However, the values of these result images are not in the range of 0-255, in order to get better images, it is advisable to adjust the initial equations.

To make the result images with standard deviation $s=25$ and mean digital data $\mu=128$, the initial equations were adapted to the L, B and V equations as follows:

$$\begin{aligned} L &= -0.171118D_1 + 1.363099D_2 + 2.014322D_3 \\ &\quad - 0.433208D_4 + 19.994065 \end{aligned} \quad (15)$$

$$\begin{aligned} B &= 1.542981D_1 + 0.733548D_2 - 0.278242D_3 \\ &\quad - 1.998286D_4 + 175.263294 \end{aligned} \quad (16)$$

Table 1. Grey level values of nine representative and typical ground features in some regions of China.

band	1. water I (clear)	2. water II turbid	4. water III River and bank	4. town	5. vegetation I :dense	6. vegetation II :densest	7. vegetation III : sparse	8. bare land I : buildings	9. bare band II : quarry
B01	30	46	37	36	41	35	49	73	79
B02	29	39	33	40	34	29	37	83	104
B03	21	31	27	27	51	38	61	48	60
B04	10	10	12	34	43	57	67	81	90
Pixels	7856	11456	5064	4899	15897	13666	12587	5600	4789

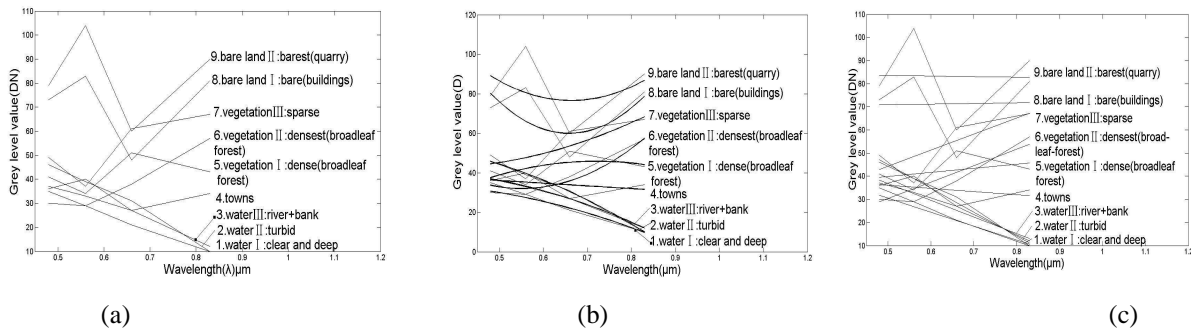


Figure1. The grey level lines, quadratic and linear curves of nine ground features. (a) Grey level curves (broken lines) of nine representative ground features, drawn according to the data in table 1. (b) Broken lines of grey level values and quadratic regression curves of nine ground features. (c) Broken lines of grey level values and linear regression curves of the nine ground features.

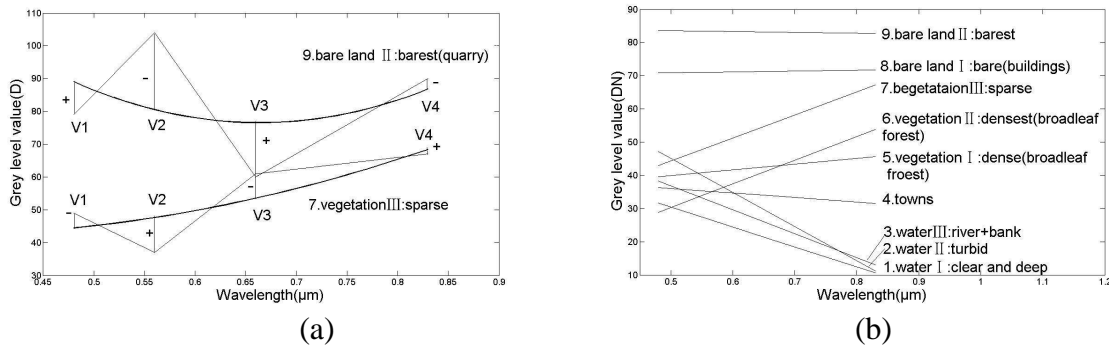


Figure2. (a) Broken lines, quadratic regression curves and regression residuals of the vegetation (7) and the bare land (9) in figure 1. (b) Linear regression curves of nine ground features from Fig.1.

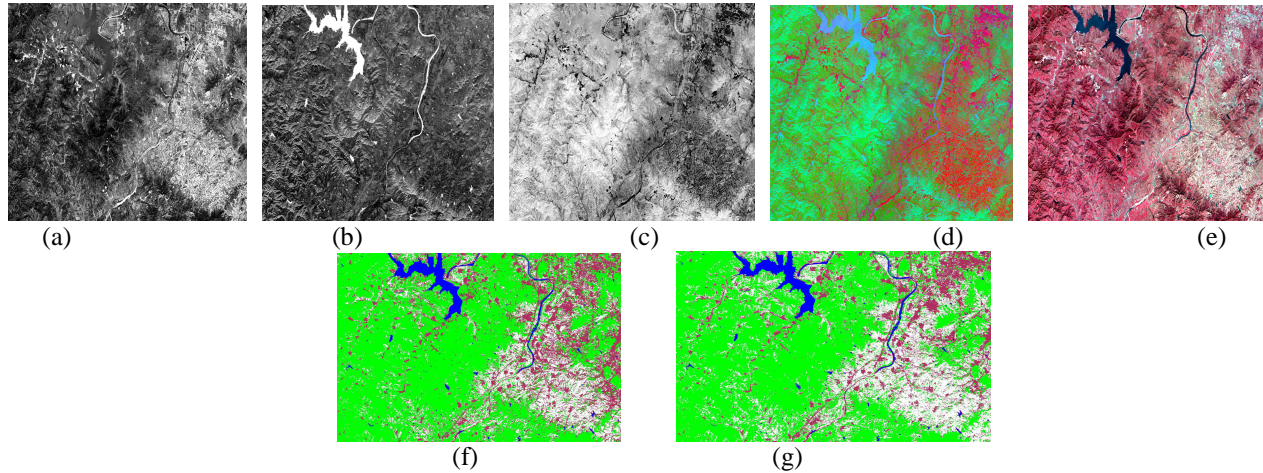


Figure 3. The result images: (a) The final L image. (b) The final B image. (c) The final V image. (d) The composite LBV image transformed from original B01, B02, B03 and B04 images. (e) The false color composite image of the B02, B03 and B04 images. (f) The classification image of the false color composite image. (g) The classification image of the transformed LBV image.

$$V = -0.437684D_1 + 1.021263D_2 - 0.720891D_3 + 0.137313D_4 + 170.888167 \quad (17)$$

4. Experiments' analysis and evaluation

Using the final transformation equations (15)-(17), the L, B, and V images can be obtained finally, and they were shown in Fig.3.

In Fig.3 (a), the grey value of the image represents the general radiance level L. The higher of the radiance lightless of the ground feature, the brighter it is in the image. Therefore, snow, cloud, and bare land including buildings, towns, and roads are bright. Meanwhile, the water is dark in the image.

In Fig.3 (b), the grey value of the image represents the visible-infrared radiation balance B. The clearer and deeper the water is, the brighter it is in the image, whereas, the vegetation is very dark.

In Fig.3(c), the grey value of this image represents the band radiance variation vector (direction and speed) V. It is can seen that, the vegetation is extremely bright in this image. Moreover, the densest vegetation owns the brightest color. However, the barest land is the darkest place in the image.

Then these black and white images were used to generate the color composite image by assigning L image red, B image blue and V image green. The composite image was shown in Fig.3 (d), and the false color composite image was shown in Fig.3 (e).

Compared to the false color composite image which only has three channels of classical method, the LBV color composite image is visually more vivid, and the ground features of the image are more enhanced especially for natural types such as soil, water and vegetation, which is helpful for the interpretation and classification of CBERS-02B images.

In order to evaluate the performance of the LBV transformed image for classification, the maximum likelihood supervise method was applied to classify both of the composite images. The classification result images were shown in Fig.3 (f) and Fig.3 (g). In these two images, the green part represents forest, the white part represents snow, the maroon part represents towns, and the blue part represents water.

For color composite image of original data, the overall classification accuracy is 63.79%, and the overall kappa statistics is 0.36. However, for the color composite image of the LBV transformed image, the overall classification accuracy is 86.21% and the overall kappa statistics is 0.71. Therefore, it is obviously seen that the classification accuracy of transformed LBV image is greatly improved than the false color composite image of original data.

5. Conclusions

In this paper, a LBV transform method for CBERS-02B images was proposed. With detailed studies on the data of t CBERS-02B and the LBV data transform equations proposed by Zeng [8], the final transformation equations for CBERS-02B images were deduced and verified. The experiment based on CBERS-02B showed that the LBV transformed images are more vivid, the features of them are more easily to classify when they were compared to the fault color composite images of original bands. The final classification accuracy of maximum likelihood supervised classification method shows that the accuracy of the LBV image is obviously better than that of the fault color composite images, which identified that the proposed LBV transformation method has good potential applications for CBERS-02B in the future.

6. Acknowledgment

The work described in this paper is supported by the projects “Aerosol Retrieval Using Remote Sensing Data Over Costal Zone Based Grid Technology” supported by NSFC, China (40801124), “Subject database of remote sensing information in coastal environment (INFO-115-C01-SDB4-17)”, “Research on key remote sensing technologies of coastal environment (No.kzcx2-yw-224)” and “Research on Novel Data Oriented SVM for Remote Sensing Information Extraction” supported by CAS, CHINA.

References

- [1] J. Zhou, D. L. Civco, and J. A. Silander, “A wavelet transform method to merge Landsat TM and SPOT panchromatic data”, *Int. J. Remote Sens.*, vol.19, no.4, pp.743-757, 1998.
- [2] P. S. Chavez and J. A. Bowell, “Comparison of the spectral information content of Landsat thematic mapper and SPOT for three different sites in the Phoenix, Arizona region”, *Photogramm. Eng. Remote Sens.*, vol.54, no.12, pp.1699-1708, 1988.
- [3] W. J. Carper, T. M. Lillesand, and R. W. Kiefer, “The use of Intensity-Hue-Saturation transform for merging SPOT panchromatic and multi-spectral image data,” *Photogramm. Eng. Remote Sens.*, vol.56, no. 4, pp. 459-467, 1990.
- [4] K. Edwards and P. A. Davis, “The use of Intensity-Hue-Saturation transformation for producing color shaded-relief images,” *Photogramm. Eng. Remote Sens.*, vol.60, no. 11, pp.1369-1374, 1994.
- [5] E. M. Schetselaar, “Fusion by the HIS transform: should we use cylindrical or spherical coordinates?,” *Int. J. Remote Sens.*, vol. 19, no.4, pp. 759-765, 1998.
- [6] J. G. Liu, “Smoothing filter-based intensity modulation: A spectral preserve image fusion technique for improving spatial details,” *Int. J. Remote Sens.*, vol.21, no. 18, pp. 3461-3472, 2000.
- [7] T. M. Tu, S. C. Su, H. C. Shyu and P. S. Huang, “A new look at IHS-like image fusion methods,” *Inf. Fusion*, vol. 2, no.3, pp. 177-186, 2001.
- [8] Zeng Zhiyuan, “A new method of data transformation for satellite images: I. Methodology and transformation equations for TM images,” *International Journal of Remote Sensing*, vol. 28, no.18, pp. 4095-4124, 2007.